TU DELFT

BACHELOR APPLIED PHYSICS

THESIS PROJECT: HANDLING BREATHING UNCERTAINTIES IN PROTON THERAPY

# The effect of breathing on dose uncertainties during proton therapy.

*Author:* Mark Arntzenius (4369831)

*Supervisor:* Zoltán Perkó

April 6, 2018

# Abstract.

Intensity Modulated Proton Therapy (IMPT) is a highly precise type of radiation therapy using protons. The dose can be delivered much more precisely than in traditional photon therapies because of protons' dose deposition, however if the protons miss the tumors because of uncertainties, organs will be damaged more easily. One of the effects that causes uncertainties in the location of the tumor is breathing. The breathing causes the tumor to move and thus dose can be delivered at surrounding organs.
IMPT delivers dose to specific spots in the tumor instead of irradiating the whole tumor at once. Thus the position of the source changes frequently. The position movement of the source and the breathing cause much dose uncertainties in the tumor.
This thesis researched how accurate one needs to approximate a breathing signal for proton therapy to acquire the same dose distribution as the measured breathing signal?
The problem is simplified to a 2D problem, only looking at one slice of the tumor. Also only 1D breathing is taken into account. Three breathing approximations are investigated. A simple, an intermediate and a complicated approximation, which are all summations of one, four and eight sines respectively. Two different tumor shapes are investigated. A square tumor and a realistic tumor. The effects of rescanning were also studied.
The thesis includes a MATLAB code which has several inputs, such as the tumor shape and the breathing signal. The output is a dose distribution in the tumor.
The dose distributions of the approximated signals are compared to the dose distribution of the measured signal. The simple approximation showed higher dose differences, meaning a worse approximation. The average error between the measured and the complicated signals' dose distributions was 5% on average for all described methods.
The approximated breathing signals have difficulty reaching some of the extreme values of the measured signal. If there are many extreme values in a short period of time, the dose distribution on the tumor has an off-set.
The intermediate and complicated approximations showed roughly the same result, meaning that approximating the breathing signal with more than four sines (intermediate) is probably not necessary.
Future research can consist of modeling a 3D problem and try different breathing approximations other than summations of sines.

# Table of Contents

# 1 Introduction

In 2012 there were 14.1 million new cancer cases and 8.2 million cancer deaths worldwide. Research states that this is only expected to grow due to growth and aging of the population [1]. There are several ways to treat cancer, for instance surgically removing the tumor or having immunotherapy. Some of these techniques are used for a long time already, whilst others are upcoming.

Radiation therapy uses high-energy particles to kill cancer cells. After a cancer cell is hit by such a particle, it will either damage the DNA structure by charged particles or by radicals. When cells' DNA is sufficiently damaged, they cannot divide themselves anymore and thus they cannot spread. Eventually they die because of the radiation and the body can break the cells down [2].

One of the upcoming techniques is IMPT (Intensity Modulated Proton Therapy). Instead of the traditional photon radiation, this therapy uses protons instead. These are used because of their dose deposition. This is a distribution which shows how the particles distribute their dose along a traveled path. An example of the dose deposition is given in Figure 1. The figure only shows the dose distribution along the depth of the body.

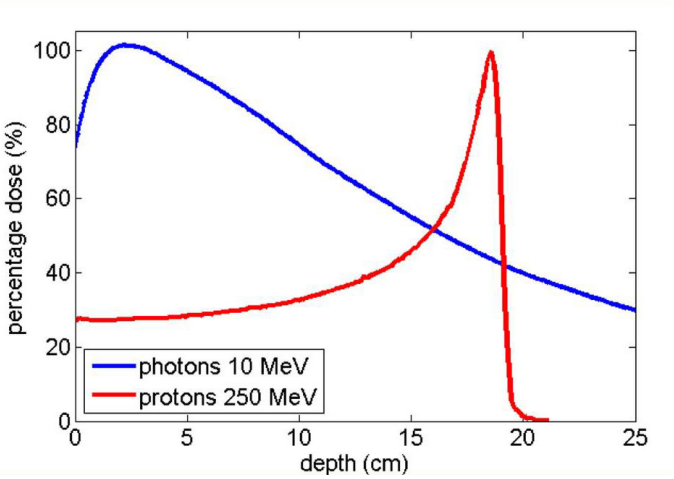


**Fig. 1:** Figure showing dose depositions of photons and protons. The blue line is the dose deposition of the photons. The red line is the dose deposition of the protons. Source: [3].

As can be seen in Figure 1, the photons distribute more dose at the entrance and the dose deposition decreases the further they travel. The dose deposition of the protons is more localized and therefore dose can be delivered much more precisely. After the peak it quickly degrades to a dose delivery of 0 Gray. This can be used to prevent the organs laying behind the tumor from being damaged.

However the preciseness also means that if the protons miss the tumor it will be heavier on the surrounding organs. Missing the tumor can happen because of uncertainties in the location of the tumor or uncertainties in the energy of the protons.

The breathing of a patient can also result in delivering dose in the wrong location, damaging surrounding organs. This thesis will look at the breathing of the patient. More specifically, how accurate does one need to approximate a breathing pattern for proton therapy to acquire the same dose distribution? A measured breathing signal is approximated in three different ways. The three approximations are compared to the measured breathing signal by making use of the dose distribution within the tumor. The dose distributions are obtained by making use of a MATLAB code. The code analyses the tumor shape and breathing motion and calculates the dose distribution on the tumor. The research examined a 2D tumor and a 1D breathing motion.

## 2 Theory

The peak of the proton dose distribution is narrow. To make sure the dose is equally distributed in the tumor a spread-out Bragg peak (SOBP) has to be made by using dose depositions from pencil beams with different energies. A pencil beam is, in this case, a beam of protons.

An SOBP tries to distribute the dose of the protons as equal as possible in the tumor. As can be seen in Figure 2, when the correct depth and amplitude is given to multiple Bragg curves, they sum up to a consistent dose throughout the tumor. The depth of the Bragg curve of protons is determined by the energy of the protons. The more energy it has, the further it can penetrate the body. The amplitude corresponds to the intensity of the pencil beam and the dose rate, the rate at which dose is received. The intensity is the time which the beam spends irradiating one particular spot.

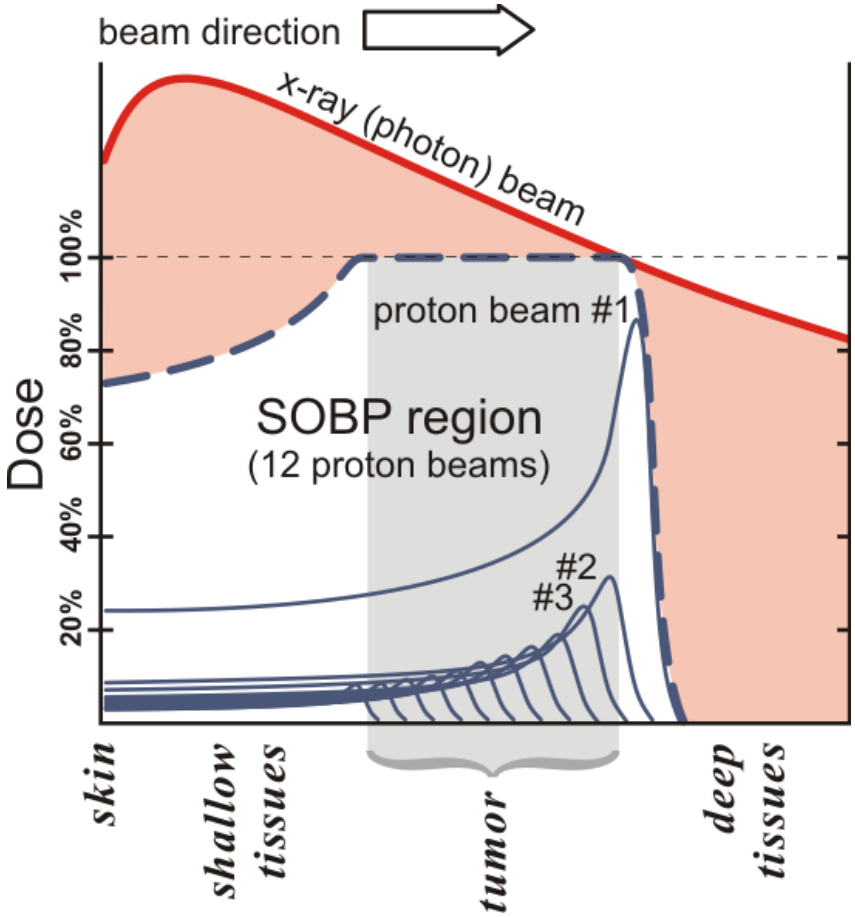


**Fig. 2:** Figure showing a spread-out Bragg curve of protons and a normal Bragg curve of photons. Source: [4]

The SOBP keeps the organs behind the tumor protected, however it does still deliver some dose in front of the tumor, see Figure 2. This means that the angle for reaching the tumor has to be chosen such that no vital or easily damaged body parts are along the path.

As protons travel, they also scatter laterally. The scattering follows a Gaussian distribution. In this case, the mean of the Gaussian is the x- and y-coordinate of the center of the source. Setting the x- and y-coordinate in the origin, Equation 1 follows.

$$f(x,y|\mu,\sigma) = \frac{1}{2\pi\sigma^2} exp\left(\frac{-(x^2+y^2)}{2\sigma^2}\right) \tag{1}$$

In Equation 1, f is the probability density function of the Gaussian spread, x and y are the coordinates of the location of interest and $\sigma$ is the standard deviation of the Gauss distribution. The standard deviation is a function dependent on the depth z, as is shown in Figure 3. The further a proton propagates the more opportunities it gets to collide with other particles and so the further it can stray from the mean. In Equation 2 this function can be seen. Since the thesis is investigating a 2D problem, the z-coordinate is chosen to have one particular value.

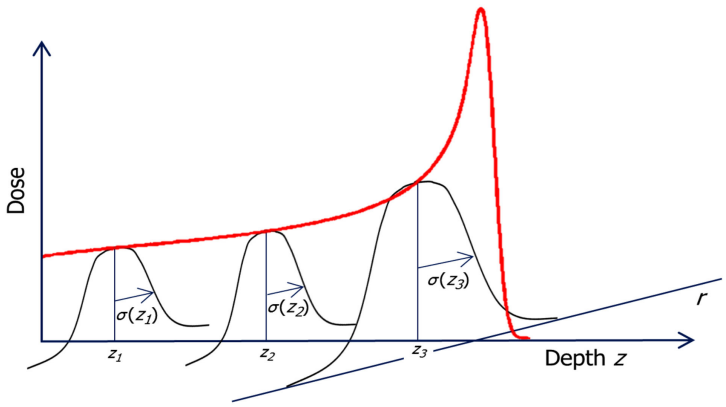


**Fig. 3:** Figure showing the three dimensional spread of protons.

In Equation 2 [5], z is the depth, R the range and $\sigma_{max}$ the maximum standard deviation. Since $0 \leq z \leq R$, the maximum standard deviation is achieved at z=R and is defined as follows, $\sigma_{max} = 0.0333R$. The range is the typically 0.8 times the maximum depth.

$$\sigma(z) = \left(0.1816\left(\frac{z}{R}\right) + 0.8184\left(\frac{z}{R}\right)^2\right) \cdot \sigma_{max} \tag{2}$$

The standard deviation of the Gaussian also has an initial spread. This is because the proton machines have an uncertainty in the starting location of the protons. The final standard deviation is a quadratic summation of the initial standard deviation and the standard deviation, which is dependent on the depth. The final equation for the standard deviation can be seen in Equation 3.

$$\sigma_{tot} = \sqrt{\sigma^2_{initial} + \sigma^2(z)} \tag{3}$$

Substituting Equation 3 in Equation 1, the Gaussian distribution in x- and y-direction arises, which is shown in Equation 4.

$$f(x, y, z|\mu, \sigma) = \frac{1}{2\pi\left(\sigma^2_{initial} + \sigma^2(z)\right)} exp\left(\frac{-\left(x^2 + y^2\right)}{2\left(\sigma^2_{initial} + \sigma^2(z)\right)}\right) \tag{4}$$

Equation 4 shows the final distribution of protons along the x,y-plane. Every proton delivers the same amount of dose, thus the equation represents the dose distribution as well, when the intensities are added to the equation.

$$D(x, y, z, x_s, y_s) = \frac{I(x_s, y_s)}{2\pi\left(\sigma^2_{initial} + \sigma^2(z)\right)} exp\left(\frac{-\left((x - x_s)^2 + (y - y_s)^2\right)}{2\left(\sigma^2_{initial} + \sigma^2(z)\right)}\right) \tag{5}$$

Equation 5 represents the dose distribution for coordinates x, y and z, where z is chosen to have one value. Because there are multiple locations from where can be shot, the coordinates $x_s$ and $y_s$ need to be taken into account. These are the coordinates of the source. $I(x_s, y_s)$ is the intensity of the source with coordinates $x_s$ and $y_s$.

The total dose on one voxel is then the dose from every source summed, shown in Equation 6.

$$D(x,y,z) = \sum_{x_s} \sum_{y_s} D(x,y,z,x_s,y_s) \tag{6}$$

All source locations have a different effect on the tumor. The higher located sources will distribute their dose on a higher part of the tumor. The treatment planning optimizes the intensities of all source locations (this will be discussed in more detail in the Model, Section 3). The dose distribution on the tumor is a summation of the dose distributions from every location.

The treatment plan is also used for moving targets, since it is not yet possible to optimize a plan for moving targets. The moving targets will have the same source locations, however the tumor will have a time dependent location. Since this thesis only looks at 1D movement, this means that in Equation 5, x becomes x(t). In the Model Section 3, a more in-depth analysis is given.

# 3 Model

The goal of the model is to calculate the dose distribution given a set of parameters. The inputs of this model are mainly the shape of the tumor and the breathing pattern. It is not yet possible to plan a treatment including the breathing. The treatment planning is done for a stationary geometry. After the planning is ready, the breathing can be added and the dose distribution including breathing motion can be calculated.

## 3.1 Treatment planning

The treatment planning creates intensities for every bixel. Bixels are elements of the bixel grid from where the protons are shot. Voxels are elements of the voxel grid whereto the protons are shot. The treatment planning also supplies a time stamp matrix which shows from which bixel the pencil beam shoots at which time.

In order to plan, the coordinate system of our setup has to be defined. The setup can be seen in Figure 4. There are two main locations to be taken into account, the starting location of the protons and their destination. The starting location is the beginning of the pencil beam, which is discretized using a bixel grid. This grid can be seen in Figure 4. The bixel grid has a total height and width of 30 mm and each bixel has a height and width of 2 mm.

The protons' destination is the tumor, which is discretized on the voxel grid. The voxel grid has the same height and width as the bixel grid. The voxels are smaller, having a height and width of 1 mm. The centers of the bixel and voxel grid align with each other. In the bottom left corner the definitions of the coordinate system can be seen (x, y and z).

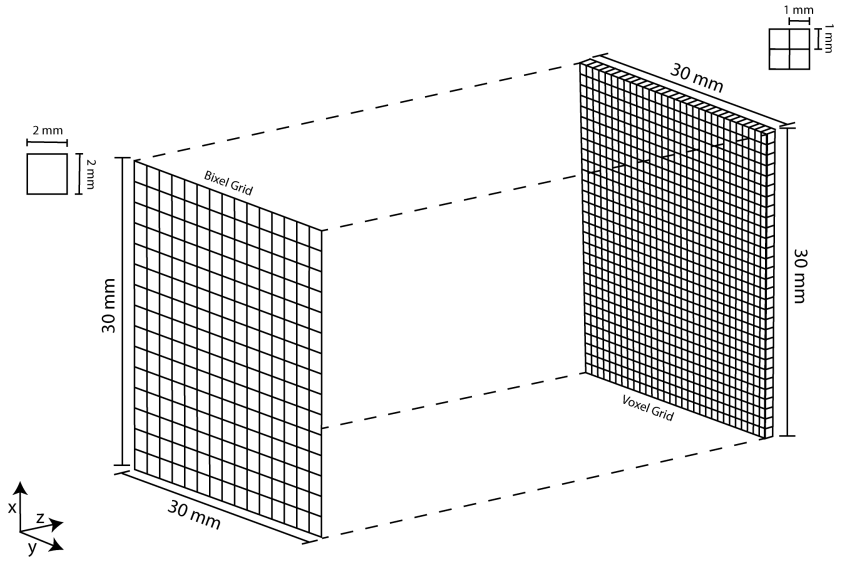


**Fig. 4:** Figure showing the setup of the proton treatment. The bixel grid is on the left and the voxel grid is on the right. In the top left corner a legend is given for the dimensions of the bixels and voxels. In the bottom left corner the definition of the coordinate system is given.

It is possible to shoot protons to the tumor from every bixel on the bixel grid. As the protons deposit dose according to the Bragg curve and scattering (as is seen in the Theory, Section 2), the difference in the bixel location and the voxel destination, together with the beam intensity, fully determines the dose in that voxel. In the model, this is a function which can be called. When several voxel doses are needed, a vector can be set as input to have several dose outputs at once.

The algorithm to calculate the dose at any voxel from any bixel can be used to create a large database. This database is called the dose deposition matrix and it contains the delivered dose values from all bixels to all voxels for unit intensities.

For every different tumor shape there is an optimal corresponding intensity map. So before the optimization begins, the shape of the tumor has to be defined. This model examines two different shapes.

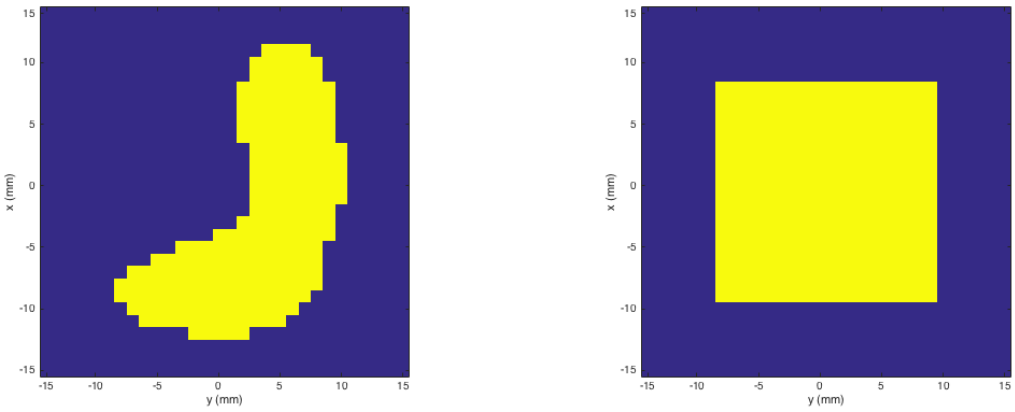


**Fig. 5:** Figures showing the examined tumor shapes. The left figure shows the realistic tumor shape. The right figure shows the examined square shape. The yellow region represents the tumor, the purple region represents the surrounding organs.

The left tumor shape shown in Figure 5 is made to look like a tumor. This particular shape is chosen, so influences in the x- and y-direction can be seen. The second shape is made as a square, shown on the right in Figure 5. The big square is chosen to highlight where the approximated breathing signals models have trouble with reconstructing the correct dose distribution.

Optimizing the intensities of the bixel grid is done by making use of the objective function shown in Equation 7.

$$f(\boldsymbol{I}) = \frac{w_t}{w_t + w_{oar}} \sum_i (\sum_j D_{i,j} I_j - D_{target})^2 + \frac{w_{oar}}{w_t + w_{oar}} \sum_k (\sum_j D_{k,j} I_j)^2 \tag{7}$$

In Equation 7, $w_t$ is the weight of importance given to the tumor, $w_{oar}$ is the weight of importance given to the organs at risk (OAR). Destroying the tumor will deliver dose to the surrounding organs. The weight of importance states how relevant it is to destroy the tumor while protecting the OAR. In this model the relative weight $\left(\frac{w_t}{w_{oar}}\right)$ is set to 650. The discussion addresses this relative weight.

The subscript j represents the bixels. The subscript i are all voxels in the tumor shape. The subscript k are all voxels outside the tumor shape. Together j and k create the whole model geometry (shown in Figure 5).

$\boldsymbol{D}$ is the dose deposition matrix (operating on voxels i and bixels j). $\boldsymbol{I}$ is the intensity vector (represented by the bold fond) containing the intensities $I_j$ corresponding to the bixels. Lastly, $D_{target}$ is the dose needed to kill the target (the tumor).

The goal of the optimization is to find the intensities $\boldsymbol{I}$, which cause f($\boldsymbol{I}$) to be as close as possible to zero. To find these intensities, the function fmincon of MATLAB is used. The fmincon function will loop through the possibilities of the intensity vector $\boldsymbol{I}$ and returns the vector $\boldsymbol{I}$, which will give the lowest value for f($\boldsymbol{I}$).

The intensity vector $\boldsymbol{I}$ represents how long the bixels have to be turned on to create the best dose distribution on the tumor. This dose distribution can then be calculated by using Equation 8. Here, $\boldsymbol{D}_{i,j}$ is the dose deposition matrix, $\boldsymbol{I}$ is the intensity vector and $\boldsymbol{D}_{delivered}$ is a vector, which contains the delivered dose on every voxel. $\boldsymbol{D}_{delivered}$ can be reshaped into a matrix so the voxels form the voxel grid.

$$\boldsymbol{D}\boldsymbol{I} = \boldsymbol{D}_{delivered} \tag{8}$$

It is impossible to shoot the protons from all the bixels at the same time, instead each pencil beam corresponding to the different bixels is used sequentially. After the intensity is reached for a bixel, the equipment has

to do some preparation to make sure the next bixel can be used. The time needed for the preparation is called the switching time $t_s$, which is in the order of milliseconds. In this code, $t_s$ 10 ms is used.

After defining $t_s$, it can be calculated at which bixel the pencil beam is at what time. It can be put in a matrix which is called the time stamp matrix. With the time stamp matrix, the breathing signal can be added correctly, as will be shown later.

$$t_j = t_{j-1} + \frac{I_{j-1}}{\dot{d}} + t_s \tag{9}$$

The general formula for calculating a time stamp $t_j$ can be seen in Equation 9. It is dependent on the previous time stamp $t_{j-1}$, the previous intensity $I_{j-1}$, the dose rate $\dot{d}$ and the switching time $t_s$. The dose rate $\dot{d}$ is set to 2 Gray per minute [6]. The dose rate is discussed in the Discussion, Section 5.

$$\boldsymbol{I} = \begin{bmatrix} I_1 = 0 \\ I_2 = 1 \\ I_3 = 4 \\ I_4 = 2 \end{bmatrix} \rightarrow \boldsymbol{T}_{stamp} = \begin{bmatrix} 0 & t_s \\ 2t_s + \frac{I_2}{\dot{d}} & 3t_s + \frac{I_2}{\dot{d}} + 4\frac{I_3}{\dot{d}} \end{bmatrix} \tag{10}$$

Equation 10 shows an example of a conversion from an intensity map $\boldsymbol{I}$ to a time stamp matrix $\boldsymbol{T}_{stamp}$. If the starting time is set to 0 seconds, the time stamp of the first bixel is 0 seconds. At the second bixel, the code checks what the intensity of the first bixel is and calculates the second value according to Equation 9.

There are different ways to move through the bixel grid with the pencil beam. Two movement methods were used. The first one can be seen in Figure 6. It is shaped in such a way that it has a consistent switching time between bixels.

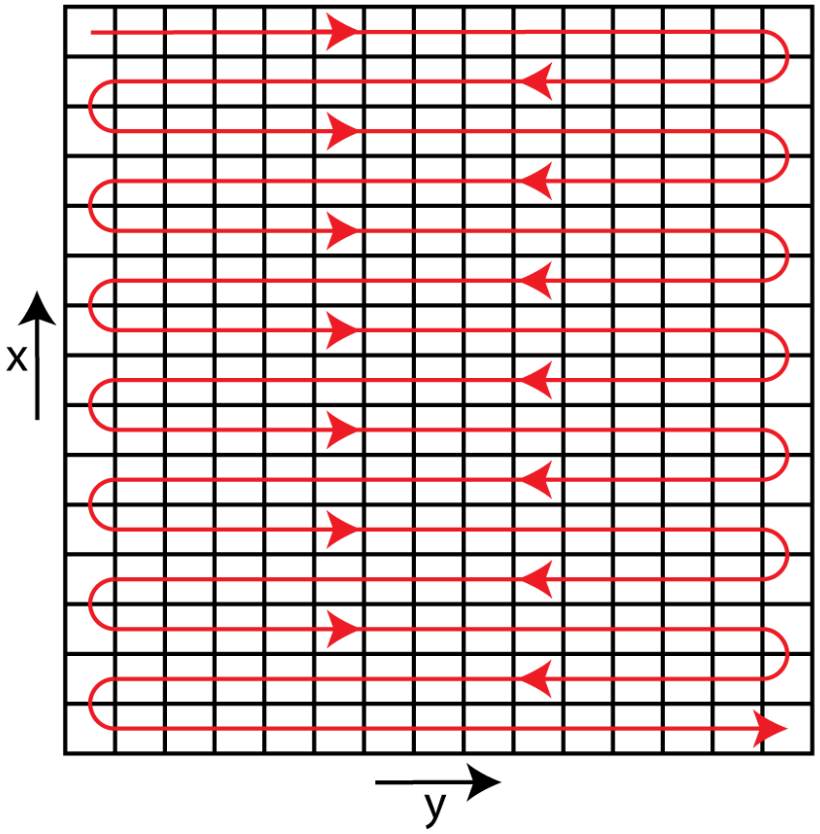


**Fig. 6:** Figure showing the route of the pencil beam through the bixel grid.

The second movement also follows the path that is illustrated in Figure 6, however it rescans. This means that the pencil beam goes through the bixel grid twice with the intensities being halved. If a spot has a particular intensity, the spot will deliver half of its intensity in the first run through the bixel grid and half of the intensity during the second run through. This method takes a longer time than the running through the bixel grid once, since twice as many switches between bixels have to be made. The advantage of going through the bixel grid twice is that extreme exhalations or inhalations during irradiation will be more likely to be canceled out.

Imagine if there was a pencil beam at a bixel, however the intensity of this bixel is very low, meaning that the time this bixels pencil beam is turned on is short. If in this short period of time the amplitude of the breathing is at its maximum (complete inhalation), all the dose which is delivered will be delivered lower than what was aimed for (since the target has moved up). However if the pencil beam moves through the bixel grid with half of the intensities, the second time the pencil beam has reached the same bixel the amplitude of breathing is not the same as the first time it passed. Now, it can be a lower amplitude, which means that not all the dose was misplaced. It can still happen that the amplitude is at its maximum again, but it is more likely the delivered dose is spread around its original target.

Both methods are shown in the Results.

## 3.2 Breathing algorithm

The breathing algorithm will alter the dose distribution according to the location of the tumor over time. The tumor has one degree of freedom in the x-direction. When the tumor has moved upwards from its original position, the pencil beam will hit below its original target.

First, the breathing pattern has to be defined. This research looks at four tumor movements. All motions are in the x-direction. Every motion is limited to a time region of 62.4 seconds, since this is the duration of the therapy session. This is calculated by making use of the highest time stamp in the time stamp matrix.

The first motion pattern is a measured signal of the displacement of a lung over time, this can be seen in Figure 7. The measurements were taken from treatments at Erasmus MC and were provided as input. The red lines and purple dotted lines shown in Figure 7 are introduced later.

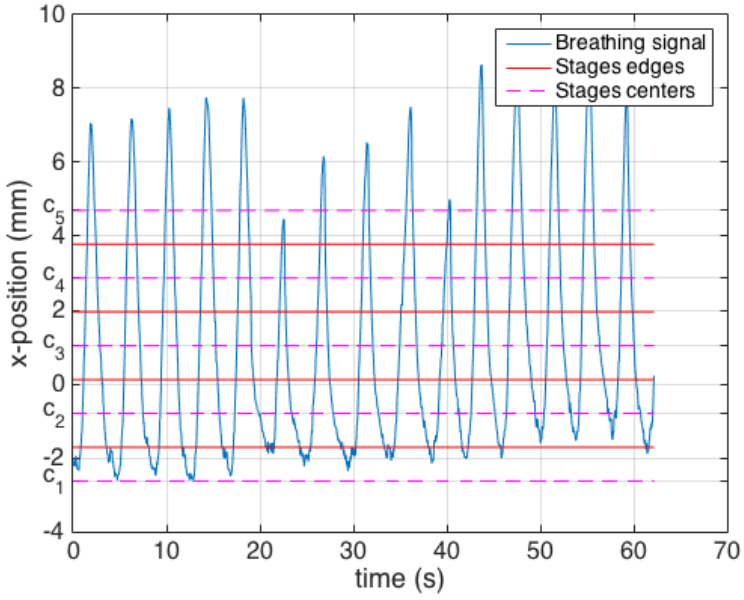


**Fig. 7:** Figure showing the measured breathing signal. The displacement of the tumor in the x-direction is displayed over time in the blue line. The red line shows the edges of the different stages. The purple dotted line are the centers of every stage.

The other three signals are approximations of this signal using sine waves. A simple, an intermediate and a complicated approximation were used. These approximations can be seen in Equations 11a, 11b and 11c accordingly.

$$x(t) = a_1 \sin(b_1 t + c_1) \tag{11a}$$

$$x(t) = \sum_{n=1}^{4} a_n \sin(b_n t + c_n) \tag{11b}$$

$$x(t) = \sum_{n=1}^{8} a_n \sin(b_n t + c_n) \tag{11c}$$

In these equations, $a_n$ is the fitted amplitude of the sine, $b_n$ is the fitted frequency and $c_n$ is the fitted phase. In Figure 8 the simple fitted curve can be seen. In Figure 9 the intermediate fitted curve can be seen. In Figure 10 the complicated fitted curve can be seen.

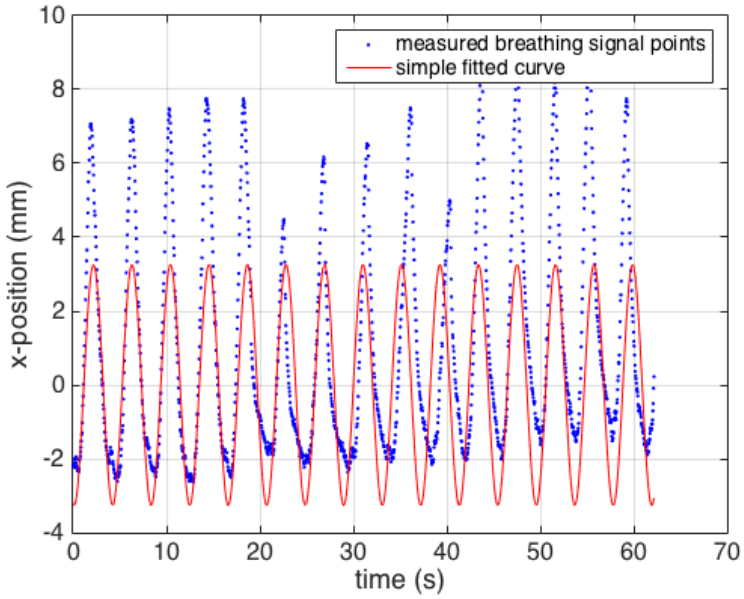


**Fig. 8:** Figure showing the simple fitted breathing signal. The displacement of the tumor in the x-direction is displayed over time. The blue dots represent the measured data points. The red line represents the simple fitted curve.

The approximations in Equations 11a, 11b and 11c are chosen to see how well of an approximation needs to be given for a similar dose distribution outcome. The approximations are optimized by means of the cftool function in MATLAB, which made use of a non-linear least squares method.

As can be seen in Figures 8, 9 and 10, the approximations have some difficulty reaching the higher x-positions of the measured signal. This is because there are more measured points in the exhalation state. The simple approximation of Figure 8 has the most difficulty with this at the beginning. It does have a better approximation in the middle region however, where the complicated approximation struggles.

Another kind of movement approximation was taken into account. The same optimizations were used and the same functions, however it was fitted to have the same average value as the measured breathing signal. By subtracting the mean of the measured signal before the optimization and adding the mean back after the optimization, such that the fitted signal had the same average value as the measured signal. The idea is that the fitted signal now can be off-set, as the measured signal is as well, and would give better results. However, this

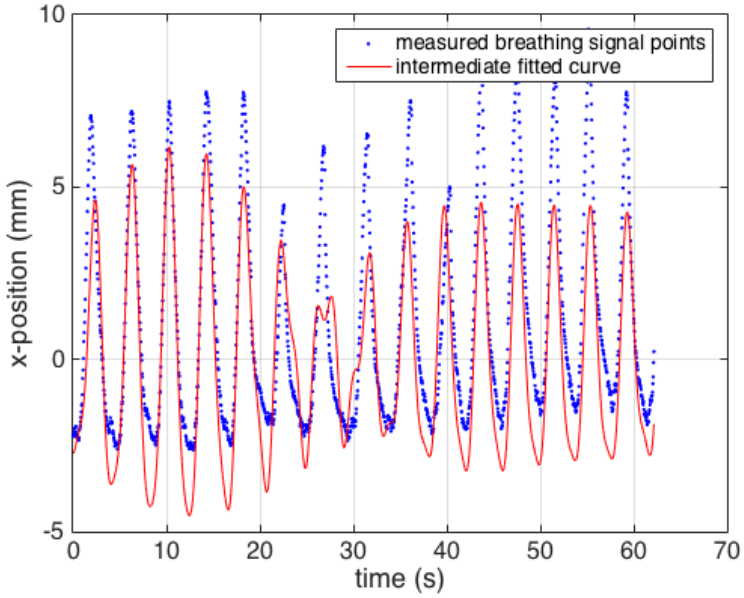


**Fig. 9:** Figure showing the intermediate fitted breathing signal. The displacement of the tumor in the x-direction is displayed over time. The blue dots represent the measured data points. The red line represents the simple fitted curve.

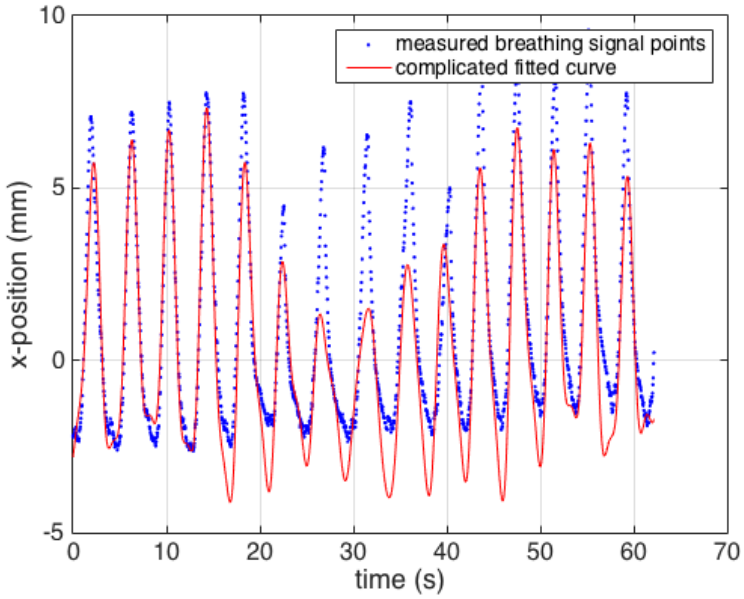


**Fig. 10:** Figure showing the complicated fitted breathing signal. The displacement of the tumor in the x-direction is displayed over time. The blue dots represent the measured data points. The red line represents the simple fitted curve.

not only resulted in an off-set for the x-position of the signal, but also for the eventual dose distribution. The distribution showed a slight offset between the fitted signal and the measured signal.

The tumor can move in increasing and decreasing x-direction, however it is not easy to correct the dose distribution according to the exact position of the tumor. If the tumor moves a small distance, the received dose

in the tumor is different from what was planned. Because it takes too much computation to calculate the dose for every tumor displacement, five stages are introduced [7].

$$c_1 = min(x(t)) \tag{12a}$$

$$c_3 = mean(x(t)) \tag{12b}$$

$$c_5 = c_3 + (c_3 - c_1) \tag{12c}$$

$$c_2 = \frac{1}{2}(c_1 + c_3) \tag{12d}$$

$$c_4 = \frac{1}{2}(c_3 + c_5) \tag{12e}$$

Each stage represents a shifted version of the tumor, representing 0%, 25%, 50%, 75% and 100% inhalation. The stages are spaced according to the mean and minimum value of the movement. In Equations 12a - 12e the calculations of the centers of every stage, as an x-coordinate, can be seen. The edges of the stages and the centers of the stages are visualized in Figure 7. The red lines represent the edges of the stages and the purple dotted lines represent the center of the stages. The average displacement of the breathing motion is the center of the third stage (as the third stage is the central stage). Equally spacing the centers every stage from another creates five stages. The space between the red lines are the stages, numbered 1 through 5 from bottom to top accordingly. The maximum value of x(t) is not taken into account because there are more measured points at a lower x-values.

Eventually, the five stages should have different dose distributions, calculated from partial intensities. The partial intensities will be determined from how much time the intensity of a bixel will spend in which stages. Adding up the dose distributions from the 5 stage results in a final dose distribution, which takes the breathing pattern into account.

Recall the time stamp matrix, which was introduced earlier in Equation 10. The matrix had a time stamp for every bixel. Since the stage is known for every time point, by looking at Figure 7, it is known how much time every bixel spends in every stage. However, there is a problem connected to this. Figure 7 is discrete, which means that the exact time points where the tumor switches between stages (crossings of the red and blue line) are probably non-existent. Using interpolation between the measurements, the exact time points can be found where the tumor switches between stages.

From this information it is possible to know what fraction of a beam intensity is delivered in what stage, thus one can define the partial intensities. The partial intensities are defined in Equation 13.

$$I_{j,s} = \frac{t_{j,s}}{t_j} I_j \tag{13}$$

In this Equation 13, $t_{j,s}$ is the time spend in stage s during the jth intensity, $t_j$ is the total time duration of the jth intensity and $I_j$ is the jth intensity.

$$\boldsymbol{D}_{delivered,s} = \boldsymbol{D}_{i,j,s}\boldsymbol{I}_s \tag{14}$$

The delivered dose in every stage can then be determined by Equation 14, where $\boldsymbol{D}_{i,j,s}$ is the dose deposition matrix of stage s and $\boldsymbol{I}_s$ is the intensity vector corresponding to stage s.

$$\boldsymbol{D}_{delivered} = \sum_s \boldsymbol{D}_{delivered,s} \tag{15}$$

The summation of the delivered dose of all stages is the final delivered dose, as is shown in Equation 15. This dose distribution including motion of the measured signal is then compared to the dose distributions of the approximated breathing signals. Also a dose-volume histogram (DVH) is calculated for every dose distribution, including the stationary case. The DVH shows how much percent of the volume of the tumor has received which dose.

# 4 Results

The results gives insight into how accurate the breathing pattern should be known to calculate an accurate dose distribution. As is discussed in the Model, Section 3, three different approximations were used for the breathing pattern (Equations 11a-11c). In the results, the dose distributions of the different approximations are shown. Also the dose volume histograms (DVH) of the distributions are shown. Furthermore the difference between the dose distribution of the approximations and the measured signal is shown. Finally, a table displays the D98 values. The D98 represents the minimum dose which at least 98% of the tumor volume receives. Results are produced for both with and without rescanning (see Figure 6).

## 4.1 Without rescanning

### 4.1.1 Dose distribution

**Square tumor**

The dose distributions for the stationary tumor and the measured breathing pattern are shown in Figure 11. As can be seen from the color pattern, the dose distribution of the stationary tumor is uniform. The measured signal has high and low dose spots. This is represented by the yellow and blue color accordingly. The color bar is given in Gray.

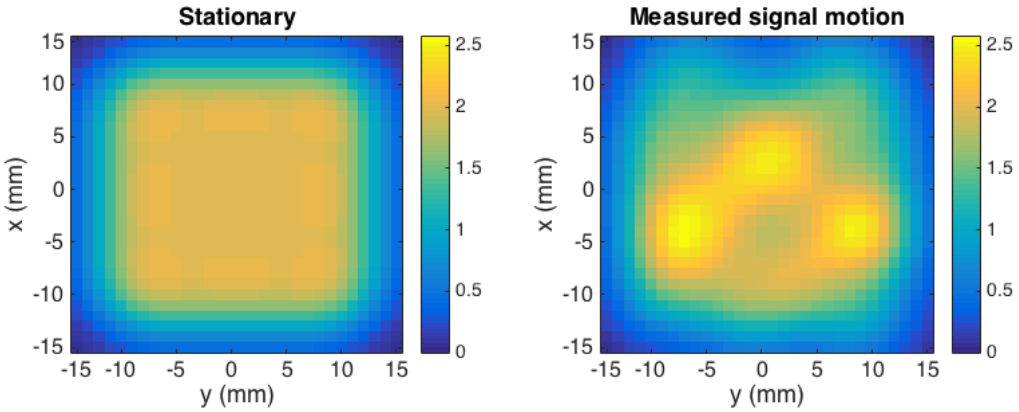


**Fig. 11:** Figure showing dose distributions for the square tumor. The left figure shows the dose distribution for the stationary tumor. The right figure shows the dose distribution for a moving tumor with the measured breathing signal. The color bar is given in Gray. The distribution is shown in y- and x-direction.

In Figure 12, the different dose distributions of the approximated breathing signals are shown. Several high and low dose spots can be recognized in these figures. The simple approximation shows to have a diagonal pattern. This can also be recognized in the other approximations, however since the simple approximation is consistent, the diagonal is easier to recognize.

**Realistic tumor**

Figures 13 and 14 address the realistic tumor. The stationary tumor and the tumor moving according to the measured signal are displayed in Figure 13. Figure 14 displays the dose distributions of the tumor moving according to the approximated breathing signals.

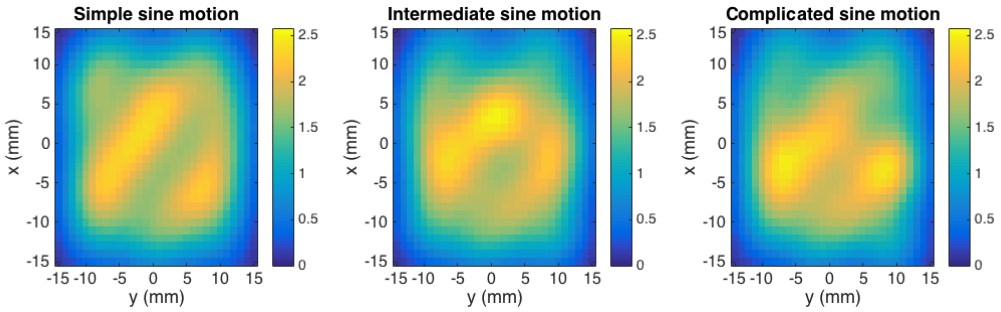


**Fig. 12:** Figure showing dose distributions for the square tumor. The left figure shows the dose distribution for a moving tumor with the simple sine approximation. The middle figure shows the dose distribution for a moving tumor with the intermediate sine approximation. The right figure shows the dose distribution for a moving tumor with the complicated sine approximation. The color bar is given in Gray. The distribution is shown in y- and x-direction.

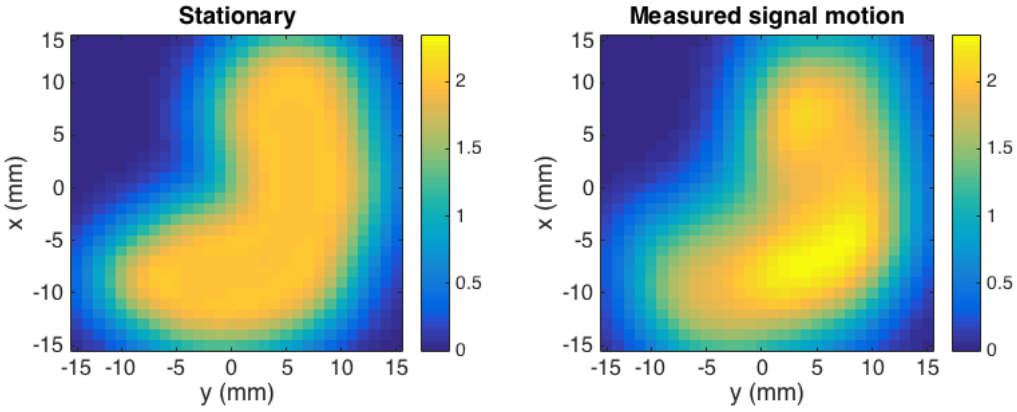


**Fig. 13:** Figure showing dose distributions for the realistic tumor. The left figure shows the dose distribution for the stationary tumor. The right figure shows the dose distribution for a moving tumor with the measured breathing signal. The color bar is given in Gray. The distribution is shown in y- and x-direction.

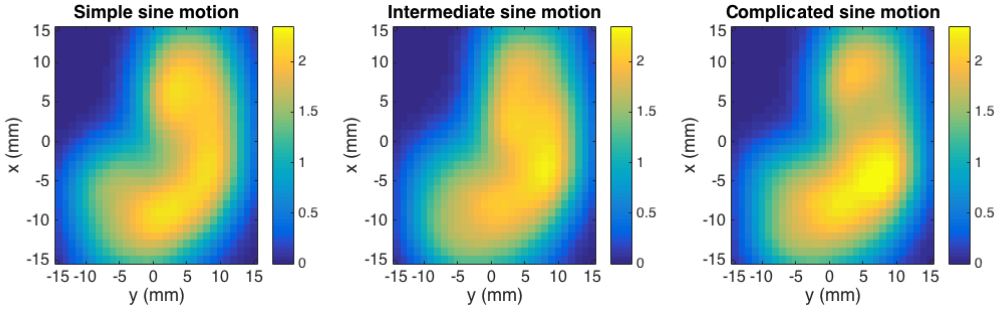


**Fig. 14:** Figure showing dose distributions for the realistic tumor. The left figure shows the dose distribution for a moving tumor with the simple sine approximation. The middle figure shows the dose distribution for a moving tumor with the intermediate sine approximation. The right figure shows the dose distribution for a moving tumor with the complicated sine approximation. The color bar is given in Gray. The distribution is shown in y- and x-direction.

### 4.1.2 Dose Volume Histogram

The DVH shows how much percent of the volume of the tumor has received which dose. It is a useful tool to assess the dose distribution as a whole. It gives a clear overview of how many percent of the volume has extreme dose values or the target dose for instance.

**Square tumor**

The DVHs of the square tumor without rescanning can be seen in Figure 15. Each line color is connected to a tumor movement, which can be seen in the legend. The measured signals' DVH is highlighted, because the approximation curves should look alike.

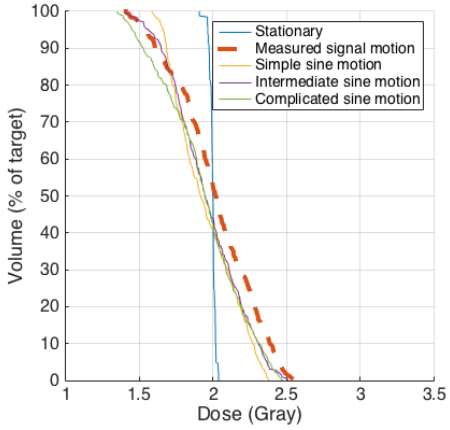


**Fig. 15:** Figure showing dose volume histogram (DVH) of the square tumor. The figure shows dose versus volume for different tumor movements.

**Realistic tumor**

The DVHs of the realistic tumor without rescanning can be seen in Figure 16. Each line color is connected to a tumor movement, which can be seen in the legend.

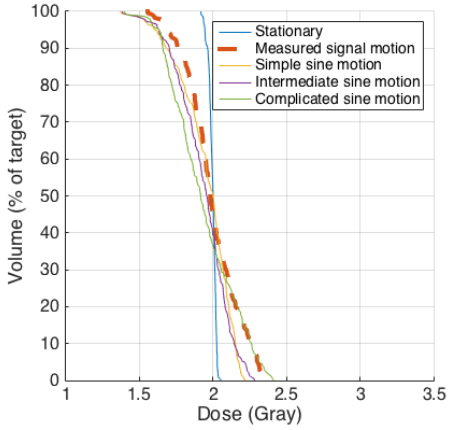


**Fig. 16:** Figure showing dose volume histogram (DVH) of the realistic tumor. The figure shows dose versus volume for different tumor movements.

### 4.1.3 Dose difference

The dose difference figures show the difference between the dose distributions of the tumor moving according to the approximated breathing signal (Figures 12 and 14) and the dose distributions of the tumor moving according to the measured breathing signal (Figures 11 and 13).

**Square tumor**

Figure 17 shows the dose difference for the square tumor. The figure shows high and low dose difference spots. Take note that the color bar has lower values compared to earlier figures, such as Figure 14.

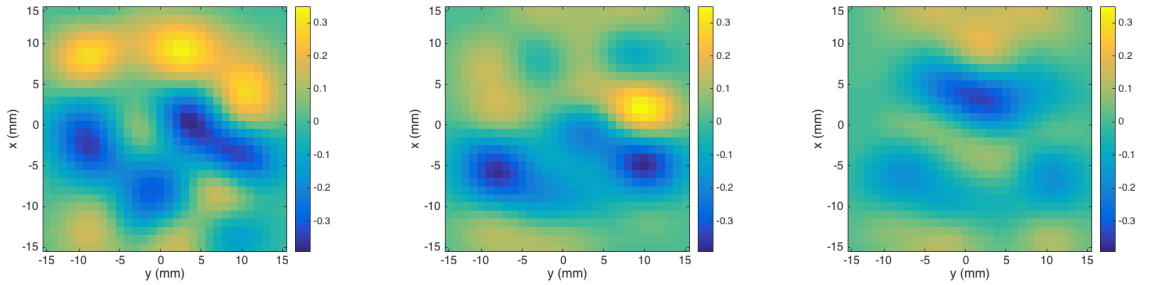


**Fig. 17:** Figures showing the difference between the dose distributions of the approximated breathing signal and the measured breathing signal of the square shaped tumor. The left figure shows the difference in dose distribution of the simple sine approximation and dose distribution of the measured breathing signal. The middle figure shows the difference in dose distribution of the intermediate sine approximation and dose distribution of the measured breathing signal. The right figure shows the difference in dose distribution of the simple complicated approximation and dose distribution of the measured breathing signal. The color bar is given in Gray. The difference is shown in y- and x-direction.

**Realistic tumor**

Figure 18 shows the dose difference for the realistic tumor. The figure shows high and low dose difference spots. The color bar has the same order of magnitude as Figure 17.

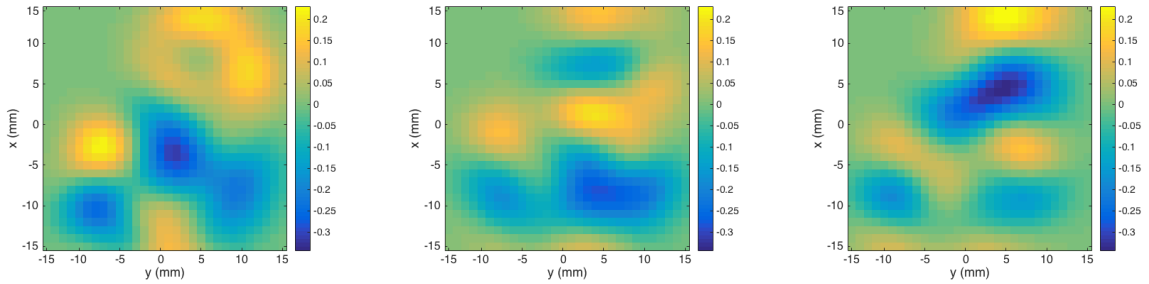


**Fig. 18:** Figures showing the difference between the dose distributions of the approximated breathing signal and the measured breathing signal of the realistic tumor. The left figure shows the difference in dose distribution of the simple sine approximation and dose distribution of the measured breathing signal. The middle figure shows the difference in dose distribution of the intermediate sine approximation and dose distribution of the measured breathing signal. The right figure shows the difference in dose distribution of the complicated approximation and dose distribution of the measured breathing signal. The color bar is given in Gray. The difference is shown in y- and x-direction.

### 4.1.4 D98 table

Table 1 shows the D98 values for the dose distributions of the different types of breathing of the square tumor. It also shows the average error between the DVH of the measured signal and the DVHs of the approximated signals. The average error is defined in Equation 16.

$$e = \frac{1}{N}\sum_{i=1}^{N} |\boldsymbol{D}_x(i) - \boldsymbol{D}_{measured}(i)| \tag{16}$$

In Equation 16, e is the error function, $\boldsymbol{D}_x$ is the dose distribution of approximation x (simple, intermediate or complicated), $\boldsymbol{D}_{measured}$ is the dose distribution of the measured signal, N is the number of voxels in the tumor and i represents a specific voxel in the tumor.

Table 2 shows the D98 value for the realistic tumor. The D98 values are ideally located at 2 Gray, because then at least 98 per cent of the tumor volume would receive the target dose.

**Table 1:** Table containing the D98 values for the dose distributions of the different breathing patterns. The average error between the DVH of the measured signal and the DVH of the approximations is also shown.

| Breathing signal type | D98 (Gray) | Average error (Gray) |
|---|---|---|
| Stationary | 1.9191 | |
| Measured | 1.5573 | |
| Simple | 1.3742 | 0.155 |
| Intermediate | 1.3876 | 0.131 |
| Complicated | 1.4021 | 0.101 |

**Table 2:** Table containing the D98 values for the dose distributions of the different breathing patterns. The average error between the DVH of the measured signal and the DVH of the approximations is also shown.

| Breathing signal type | D98 (Gray) | Average error (Gray) |
|---|---|---|
| Stationary | 1.9087 | |
| Measured | 1.4096 | |
| Simple | 1.5864 | 0.105 |
| Intermediate | 1.4024 | 0.122 |
| Complicated | 1.3527 | 0.105 |

According to the average errors in Table 1, it can be concluded that the complicated approximation is closest to the measured signal. This is in agreement with Figure 17, where the complicated approximation is the most uniform and has the least high and low dose spots compared to the other approximations.

From the average errors shown in Table 2, the intermediate approximation has the highest average error. Looking at Figure 18, this is not obvious. The average errors are a measure of how good the approximation is at the tumor. The surrounding organs are not taken into account here since the tumor is focused on. Even though the intermediate approximation may seem like it is just as good as the other approximations, its high and low dose spots are only located in the tumor. The other approximations also show high and low dose spots in the surrounding organs and less spots within the tumor.

The average errors of the realistic tumor show to be lower than the average errors of the square tumor. Since the square tumor is bigger, it has more volume to distribute dose to, which means that the summation of intensities of all bixels is higher for the square tumor. The breathing has more effect on the square tumor simply because there is more to irradiate. As the approximations are not perfect, their weaknesses have more chances to show themselves in the square tumor, since there is more irradiation involved.

## 4.2 With rescanning

### 4.2.1 Dose distribution

**Square tumor**

In Figure 19 the dose distributions of the stationary tumor and the measured breathing pattern are shown. Compared to Figure 11, there are less high dose spots.

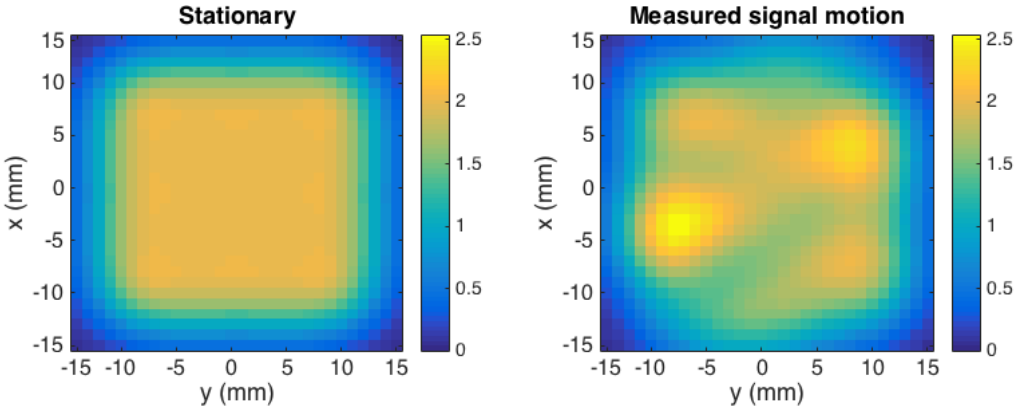


**Fig. 19:** Figure showing dose distributions for the square tumor. The left figure shows the dose distribution for the stationary tumor. The right figure shows the dose distribution for a moving tumor with the measured breathing signal. The color bar is given in Gray. The distribution is shown in y- and x-direction.

In Figure 20, the different dose distributions of the approximated breathing signals are shown. Several high and low dose spots can be recognized in these figures. These are all around the same location regardless of the breathing signal approximation. However the dose values of these spots differ.

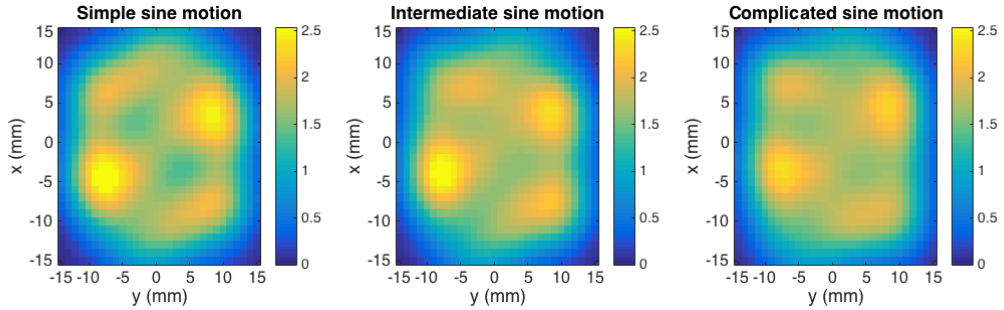


**Fig. 20:** Figure showing dose distributions for the square tumor. The left figure shows the dose distribution for a moving tumor with the simple sine approximation. The middle figure shows the dose distribution for a moving tumor with the intermediate sine approximation. The right figure shows the dose distribution for a moving tumor with the complicated sine approximation. The color bar is given in Gray. The distribution is shown in y- and x-direction.

### 4.2.2 Realistic tumor

The following figures address the realistic tumor. The stationary tumor and the tumor moving according to the measured signal are displayed in Figure 21. Figure 22 displays the dose distributions of the tumor moving according to the approximated breathing signals. Here some differences occur between the three figures. The high dose spots aren't the same for every approximation. Purely looking at the high dose locations, the complicated approximation looks like the measured breathing signal.

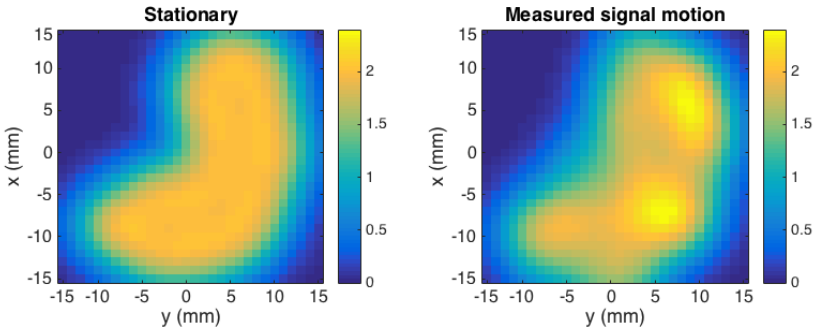


**Fig. 21:** Figure showing dose distributions for the realistic tumor. The left figure shows the dose distribution for the stationary tumor. The right figure shows the dose distribution for a moving tumor with the measured breathing signal. The color bar is given in Gray. The distribution is shown in y- and x-direction.

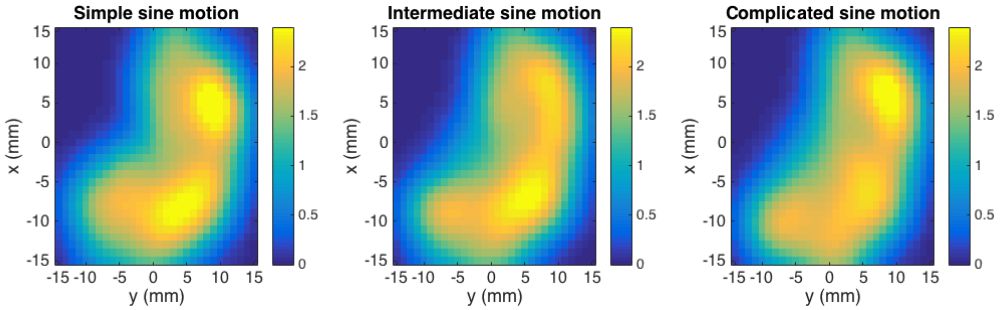


**Fig. 22:** Figure showing dose distributions for the realistic tumor. The left figure shows the dose distribution for a moving tumor with the simple sine approximation. The middle figure shows the dose distribution for a moving tumor with the intermediate sine approximation. The right figure shows the dose distribution for a moving tumor with the complicated sine approximation. The color bar is given in Gray. The distribution is shown in y- and x-direction.

### 4.2.3 Dose Volume Histogram

**Square tumor**

The DVHs of the square tumor with rescanning can be seen in Figure 23. Each line color is connected to a tumor movement, which can be seen in the legend.

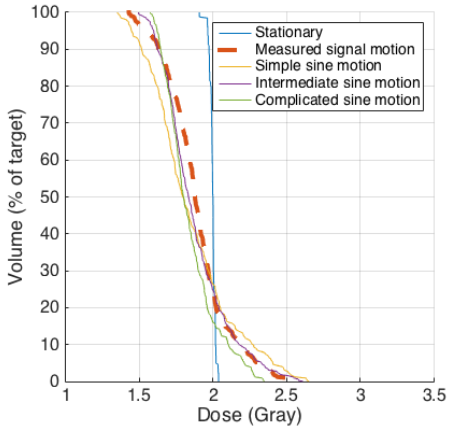


**Fig. 23:** Figure showing dose volume histogram (DVH) of the square tumor. The figure shows dose versus volume for different tumor movements.

**Realistic tumor**

The DVHs of the realistic tumor with rescanning can be seen in Figure 24. Each line color is connected to a tumor movement, which can be seen in the legend.

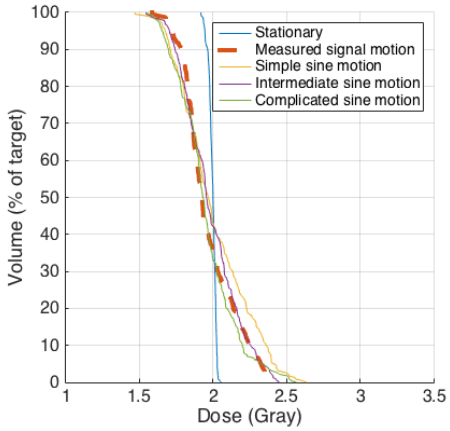


**Fig. 24:** Figure showing dose volume histogram (DVH) of the realistic tumor. The figure shows dose versus volume for different tumor movements.

Comparing Figure 23 to Figure 15, some differences can be found. Figure 23 is much steeper at the beginning. It is also more centered around the 2 Gray, which is to be expected since there are less extreme values. However Figure 16 is more centered around 2 Gray than Figure 24. This is because Figure 22 shows more high dose locations compared to Figure 14.

## 4.3 Dose difference

The dose difference figures show the difference between the dose distributions of the tumor moving according to the approximated breathing signal (Figures 20 and 22) and the dose distributions of the tumor moving according to the measured breathing signal (Figures 19 and 21).

### 4.3.1 Square tumor

Figure 25 shows the dose difference for the square tumor. The figure shows high and low dose difference spots. Take note that the color bar has lower values compared to earlier figures, such as 22. As can be seen, this is much more uniform than Figure 17. The intermediate approximation seems to be the most uniform and thus have the least difference to the measured signal. The simple approximation has many weak spots, most of which are on the left side of the tumor. The dose difference values are much smaller as well, depicted by their blue green color.

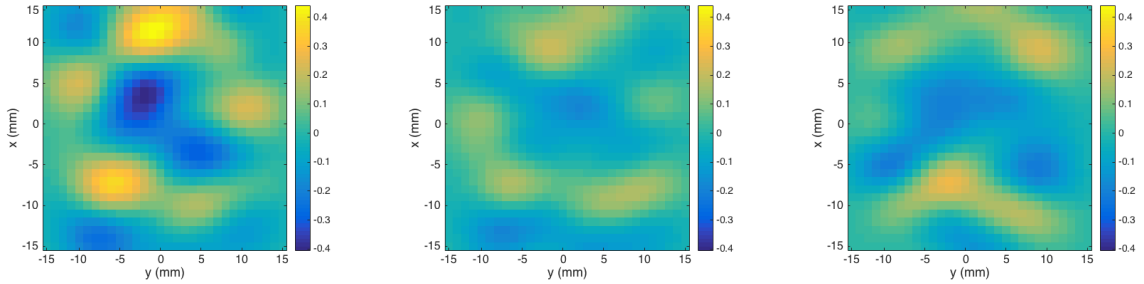


**Fig. 25:** Figures showing the difference between the dose distributions of the approximated breathing signal and the measured breathing signal of the square shaped tumor. The left figure shows the difference in dose distribution of the simple sine approximation and dose distribution of the measured breathing signal. The middle figure shows the difference in dose distribution of the intermediate sine approximation and dose distribution of the measured breathing signal. The right figure shows the difference in dose distribution of the simple complicated approximation and dose distribution of the measured breathing signal. The color bar is given in Gray. The difference is shown in y- and x-direction.

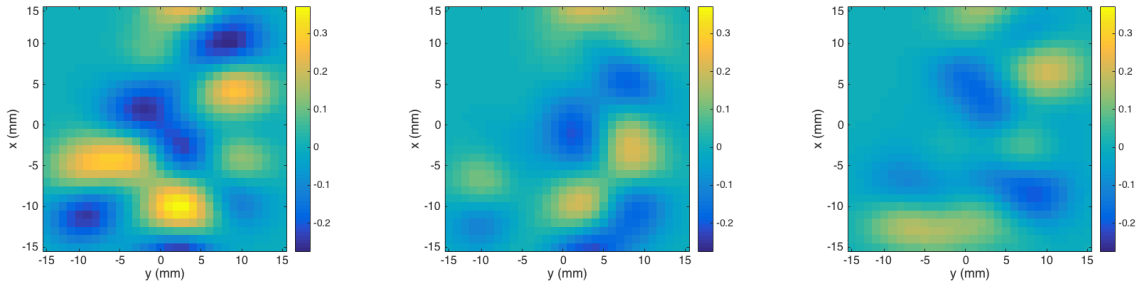


**Fig. 26:** Figures showing the difference between the dose distributions of the approximated breathing signal and the measured breathing signal of the realistic tumor. The left figure shows the difference in dose distribution of the simple sine approximation and dose distribution of the measured breathing signal. The middle figure shows the difference in dose distribution of the intermediate sine approximation and dose distribution of the measured breathing signal. The right figure shows the difference in dose distribution of the simple complicated approximation and dose distribution of the measured breathing signal. The color bar is given in Gray. The difference is shown in y- and x-direction.

### 4.3.2 Realistic tumor

Figure 26 shows the dose difference for the realistic tumor. The figure shows high and low dose difference spots. The color bar has the same order of magnitude as Figure 25. Also here the simple approximation has more high and low dose spots. The dose difference values are much smaller than in Figure 18. The rescanning has reduced the difference in the dose distributions of the measured signal and the approximated signals.

Table 3 shows the D98 values for the dose distributions of the different types of breathing of the square tumor. It also shows the average error between the DVH of the measured signal and the DVHs of the approximated signal. Table 4 shows the D98 value for the realistic tumor and the average error.

**Table 3:** Table containing the D98 values for the dose distributions of the different breathing patterns. The average error between the DVH of the measured signal and the DVH of the approximations is also shown.

| **Breathing signal type** | **D98 (Gray)** | **Average error (Gray)** |
|---|---|---|
| Stationary | 1.9191 | |
| Measured | 1.5573 | |
| Simple | 1.3742 | 0.154 |
| Intermediate | 1.3876 | 0.078 |
| Complicated | 1.4021 | 0.119 |

**Table 4:** Table containing the D98 values for the dose distributions of the different breathing patterns. The average error between the DVH of the measured signal and the DVH of the approximations is also shown.

| **Breathing signal type** | **D98 (Gray)** | **Average error (Gray)** |
|---|---|---|
| Stationary | 1.9087 | |
| Measured | 1.4096 | |
| Simple | 1.5864 | 0.119 |
| Intermediate | 1.4024 | 0.081 |
| Complicated | 1.3527 | 0.065 |

The average errors of Table 3 are comparable to Table 1, however the intermediate approximation has decreased. The average errors of Table 4 are also comparable to the values of Table 2. The intermediate and the complicated approximations have decreased this time. The intermediate approximation benefits most from the rescanning.

The average errors of Table 4 are lower than the average errors of Table 3, this is also due to the fact that the square tumor is bigger than the realistic tumor.

# 5 Discussion

## 5.1 2D tumor

The tumor is obviously a 3D object, however in this thesis only a slice of the tumor is examined. This slice is portrayed as a 2D object.

The relative weight of importance, discussed in the model (Equation 7), becomes abnormally high due to the 2D problem. The organs at risk (OARs) take up a higher volume percentage in a 2D problem than 3D. This means the OARs influence the problem a lot more, resulting in a higher relative weight, which was shown in Equation 7.

The dose rate is the rate at which dose is received in the tumor. Since this is a 2D problem, the volume of the tumor has decreased, as only one slice of the tumor is examined. The research tried to look at a realistic therapy time to examine and also a realistic received dose. Since the volume has decreased ($V \propto M$), the therapy time has stayed the same and the dose rate ($= \frac{D_{received}}{t_{therapy}} = \frac{E_{received}}{Mt_{therapy}}$) stayed the same, it means that the rate at which protons are shot from the source has to be decreased as well. The rate at which protons are shot has decreased with the same factor as $\frac{V_{2D}}{V_{3D}}$.

Also because it is only a 2D problem, the distribution in the z-direction doesn't matter since the dose rate is adjusted to fit to a single slice of the tumor. The Bragg curve and spread-out Bragg curve are therefore not included in this research. A 3D problem definitely must include these factors.

## 5.2 Approximated signals

Figures 8, 9 and 10 show the approximated signal which were used. All approximations have difficulty achieving the high peaks of measured points. Since a non-linear least squares method was used, every measured point has the same weight. The measured signal spends more time in exhale than in inhale, thus the fitted curves tend to be on the lower x-positions. The rescanning tries to cope with the badly approximated high x-positions, as is described at the end of Section 3.1.

The complicated approximation of the breathing signal approximates the measured breathing signal well at beginning. However in the middle it has some trouble (see Figure 10). Within this time region the pencil beam has moved through the bixel grid. The voxels, which align with these bixels, and the voxels around those have different dose distribution since the x-position is estimated badly.

## 5.3 Dose distribution

The high and low dose spots in Figure 12 are located around the same locations. The shape can also be recognized in other dose distributions. The high dose locations seem to form a diagonal shape. These diagonals that are formed are a result from the movement of the pencil beam through the bixel grid (Figure 6). When the breathing signal moves up- and downwards periodically and the pencil beam moves through the bixel grid, one can imagine that the combined movement can interfere along the diagonals, creating high and low dose locations along diagonals. As the movement of the simple sine is more consistent, the diagonals are more clear compared to a more complicated motion.

As can be seen in Figure 12 and 14, the dose on the tumor can be as high as 2.5 Gray, which is 25% above the target dose of 2 Gray. This is a result of the diagonals. This is also why in Figure 15 and 16 the lines aren't as steep as the stationary tumors' DVH.

Rescanning does a better job at uniformly distributing the dose. The high and low dose regions get canceled out more easily, because maximums and minimums of breathing amplitudes have a higher chance of being avoided.

## 5.4 Dose difference

The dose difference depicted in Figures 17, 18, 25 and 26 have high and low dose spots. These are widely spread among the tumor, no real pattern is to be recognized. The locations of the high and low dose spots are related to the time stamps where the approximations have trouble recreating the measured signal (see Figures 8, 9 and 10). The dose is then delivered lower than which was to be expected, however since this happens frequently this is not very apparent in the final dose difference.

# 6 Conclusion

The goal was to determine how accurately the breathing signal had to be known such that the dose distributions were alike. The three approximations showed that a much too simple approximation had difficulties, since the maximums and minimums of the breathing amplitude are harder to reach. This resulted in differences up to 0.3 Gray on the dose distributions of the measured signal and the simple approximated signal, see Figure 25.

The average errors mentioned in Tables 1, 2, 3 and 4 showed that the complicated approximation had the lowest average error values, except for the square tumor with rescanning. From these average errors it can be concluded that the complicated error results in a better dose distribution.

The differences between the complicated and the intermediate approximation of the average errors are roughly 0.02 Gray (see Tables 1, 2, 3 and 4). Since the target dose was 2 Gray, this is roughly a 1% difference, which is small. The differences between the complicated and the simple approximation of the average error are roughly 0.04 Gray, which equals 2%. Since the complicated approximation is not harder to acquire there is no reason not to use it.

The simplifications of the problem had a big influence on the research. A 2D tumor versus a 3D tumor and a 1D breathing motion versus a 3D motion brings a lot of new factors to take into account. Before the results of this thesis can be used, the higher dimensional research has to be done.

The future research should therefore expand in multiple breathing directions and a 3D tumor. Also a different approach on approximations can be made. In this thesis it was assumed the breathing signal was a sine summation, however other approximations are also valid. Multiple routes through the bixel grid with the pencil beam can also be investigated. Rescanning showed a great difference in result. One can imagine a third time could also improve.

Ultimately an optimization of the intensities should be done with the breathing motion taken into account. A realization of this is however too far fetched currently.

# References


1. National Cancer Institute. Radiation therapy for cancer. https://www.cancer.gov/about-cancer/understanding/statistics, March 2017.
2. National Cancer Institute. Radiation therapy for cancer. https://www.cancer.gov/about-cancer/treatment/types/radiation-therapy/radiation-fact-sheetr1, June 2010.
3. Swiss Physical Society. Modern techniques in radiation oncology. https://www.sps.ch/en/articles/progresses/modern-techniques-in-radiation-oncology-36/, nov 2013.
4. David Jette and Weimin Chen. Creating a spread-out bragg peak in proton beams. Institute of Physics and Engineering in Medicine, may 2011.
5. Martijn Engelsman Wilhelm Wouters, Danny Lathouwers. *Medical Physics of photon and proton radiotherapy*. Delft University of Technology, apr 2016.
6. W.-C. Hsi C. E. Allgower F. Jesseph A. N. Schreuder J. B. Farr, A. E. Mascia and M. Wolanski. Clinical characterization of a proton beam continuous uniform scanning system with dose layer stacking. Indiana University, Department of Physics, nov 2008.
7. Dominique Reijtenbagh. Simulation and quantification of the interplay effect in treatment of lung tumors with impt. Master's thesis, Delft University of Technology, jul 2017.